

Polar relaxation mode in pure and iron-doped barium titanate

M. Maglione

Laboratoire de Physique du Solide, Université de Bourgogne, 21004 Dijon, France

R. Böhmer and A. Loidl

Institut für Physik, Universität Mainz, 6500 Mainz, Federal Republic of Germany

U. T. Höchli

IBM Research Division, Zurich Research Laboratory, 8803 Ruschlikon, Switzerland

(Received 7 August 1989)

A dielectric relaxation peak is reported in BaTiO₃ and BaTi_{1-x}Fe_xO₃. It is nearly monodisperse, centered in the 10⁸-Hz range, and slowest at the transition temperature $T_c \approx 413$ K from the cubic to the tetragonal phase. Iron doping lowers T_c and slows down this relaxation mode.

I. INTRODUCTION

The soft-mode concept is most often quoted for the cubic-to-tetragonal transition of BaTiO₃ implying coherent, phononlike motion of Ti⁴⁺ ions with respect to their oxygen cages.¹ However, an x-ray determination of the BaTiO₃ structure revealed unmistakable signs of disorder in the cubic, in the tetragonal, and in the orthorhombic phase.² The microscopic structure in the cubic phase was described in terms of polar correlations extending from 40 to 100 Å, suggesting that the cubic-to-tetragonal transition may have an order-disorder character.³ X-ray and neutron data⁴ provided no quantitative information on the possible dynamics of this disorder.⁵ Guided by the observation that the soft mode was strongly overdamped near the cubic-to-tetragonal transition temperature T_c and several suggestions^{1,6} that this might be due to double-well potentials at Ti sites, we searched for dielectric relaxation in a hitherto unaccessed frequency range.⁷ Our discovery of the strongest relaxation mode at 10⁸ Hz determines the nature of disorder seen in 1968 and gives some clues as to its origin.

II. EXPERIMENT

Pure and Fe-doped BaTiO₃ crystals were grown at the Université de Bourgogne using the Czochalsky pulling method. From the same boule, we obtained 0.5-cm³ samples used for optical investigations and smaller 5-mm³ samples used in the present study. Pure BaTiO₃ samples were also purchased from J. Albers of the Universität des Saarlandes. These samples have their faces parallel to the [100] crystallographic plane. Two opposite faces of the cubic-shaped samples were electroded by gold.

The complex impedance of the sample was recorded with an HP 4191A impedance analyzer, with a test frequency range between 1 MHz and 1 GHz. The sample temperature was controlled with an accuracy of better than 0.1 °C from room temperature up to 473 K. A specially constructed radio-frequency conductor connected the output port of the impedance analyzer with the sample

in the oven.⁸

In this setup the sample is considered to be a lossy capacitor with lumped-circuit capacitance $C = C_0 \epsilon_1$ and conductance $G = (\omega C_0)^{-1} \epsilon_2$. Here, C_0 is the empty-cell capacitance and ω is the angular frequency. The impedance characteristics were converted directly into real and imaginary parts of the dielectric susceptibility $\epsilon^* = \epsilon_1 + i\epsilon_2$. The representation of the sample in terms of C and G requires that its dimensions are much smaller than the wavelength of light, which in a sample with $\epsilon = 1000$ is 1 cm at 1 GHz. To keep the contribution of surface layers low and to meet the above requirements, samples were cut to approximately cubic shape. Even so, the frequency range was sometimes limited to 250 MHz.⁹

Figure 1 shows the frequency dependence of the real (upper frame) and imaginary (lower frame) part of ϵ^* for pure BaTiO₃ at temperatures above and below the cubic-to-tetragonal phase transition ($T_c = 413$ K). The high transition temperature is taken as an indication of the purity of the sample. A mere 75-ppm Fe reduces T_c to 408 K. The results of a fit to

$$\epsilon^* = \epsilon_\infty + (\epsilon_s - \epsilon_\infty) \int g(\tau) d\tau / (1 + i\omega\tau)$$

are indicated by the solid lines in Fig. 1. Here $g(\tau)$ is derived from a log-normal distribution of relaxation times of width $\Delta(\ln\tau)$,

$$g(\tau') = \frac{1}{[2\pi\Delta(\ln\tau)]^{1/2}} \exp\{-[(\ln\tau' - \ln\tau)/\Delta(\ln\tau)]^2\}. \quad (1)$$

When $\Delta(\ln\tau)$ approaches 0, then $g(\tau_0)$ approaches $\delta(\tau)$ and the customary Debye expression is recovered. Thus, $\Delta(\ln\tau)$ is a measure of the deviation from Debye behavior, i.e., polydispersion.¹⁰ In all our samples, the values for $\Delta(\ln\tau)$ are less than one. The polydispersive parameter $\Delta(\ln\tau) \sim 1$ means that the relaxation time distribution is as wide as half a decade. Since it does not depend markedly on T we concentrate on the parameters ϵ_s , ϵ_∞ , and τ describing the size and the leading rate of Debye relaxation. Relaxation behavior of doped BaTiO₃ is shown in Fig. 2.

Figure 3 shows the value of dispersion step $\epsilon_s - \epsilon_\infty$

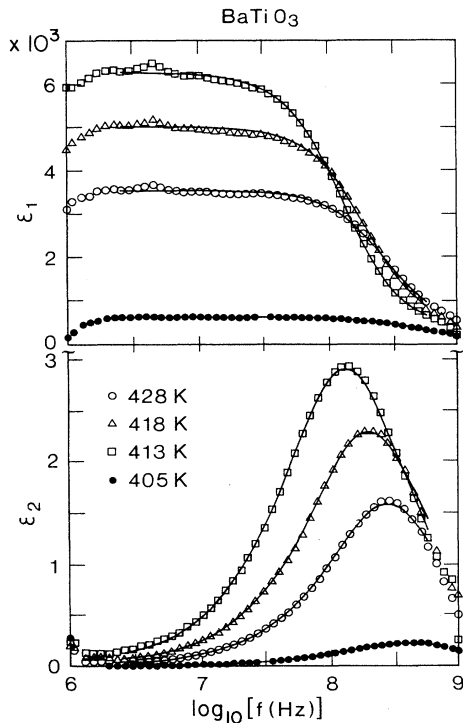


FIG. 1. Dielectric susceptibility $\epsilon^* = \epsilon_1 - i\epsilon_2$ of BaTiO_3 vs frequency. Solid curves: fit to

$$\epsilon^* = \epsilon_\infty + \int g(\tau) d\tau (\epsilon_s - \epsilon_\infty) / (1 + i\omega\tau),$$

where $g(\tau)$ is a Gaussian distribution of logarithmic relaxation times [see Eq. (1)]. For $T = 413$ K, we find that $\epsilon_\infty = 5 \times 10^2$, $\epsilon_s = 6 \times 10^3$, $(2\pi\tau)^{-1} = 10^8$ Hz, and the width of the Gaussian is $\Delta(\ln\tau) = 0.2 \pm 0.2$. Further results are found in the text and plotted in Figs. 3 and 4.

versus temperature for several crystals. We note that $\epsilon_s - \epsilon_\infty$ of the pure crystal corresponds to the value of $\epsilon(\omega)$ found in the literature, indicating that no dispersion occurs between our lowest frequency (1 MHz) and the literature values, usually 1 kHz,¹¹ and that ϵ_∞ is much smaller than ϵ_s .

In all cases studied, there is one predominant relaxation rate τ^{-1} , or inverse relaxation time τ , associated with the dispersion regime (Fig. 4). We note that τ^{-1} ranges from 10^7 to 10^9 s⁻¹ and drops sharply at the same T_c at which the static susceptibility is maximum. Iron doping enhances the maximum susceptibility near T_c , shifts T_c to a lower value,¹² and has a tendency to enhance the distribution width $\Delta(\ln\tau)$ as well. Dielectric susceptibilities have also been reported^{13,14} for GHz frequencies on flux-grown BaTiO_3 containing impurities.¹¹ These techniques imply a determination of a phase shift $\Delta L/\lambda_0$ due to insertion of a sample in a microwave lead. ΔL is the shift of the wave pattern in meters, λ_0 is its wavelength. Its characteristics are obtained from the relation¹⁵

$$\tan[\pi(d + \Delta L)/\lambda_0] = \sqrt{\epsilon_1} \tan(\pi d \sqrt{\epsilon_1}/\lambda_0).$$

The postulate of unambiguity and precision considerations

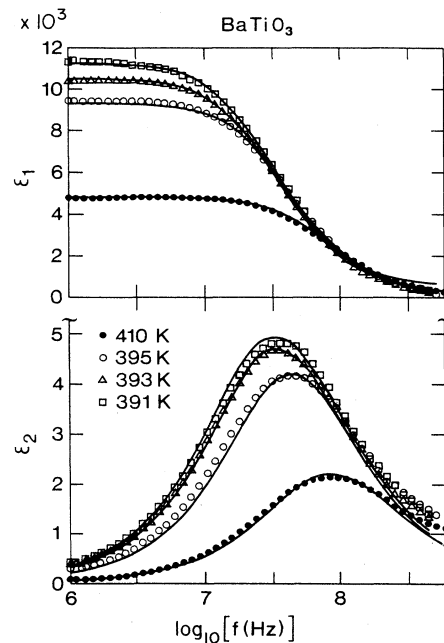


FIG. 2. Dielectric susceptibility for BaTiO_3 doped with 0.9% Fe for different temperatures above $T_c = 391$ K. Values of parameters $\epsilon_s - \epsilon_\infty$ and τ_0 are plotted in the following figures. In all cases, $\Delta(\ln\tau) < 1$. See text.

limit sample dimensions to $d\lambda_0/4\sqrt{\epsilon_1}$, similar to the case for the lumped-circuit conditions. This condition is not met for the data reported at GHz frequencies¹³ in the temperature range near T_c where ϵ is large.

III. INTERPRETATION

The picture which evolves on the basis of these findings is a nearly monodispersive relaxation slowing down at T_c

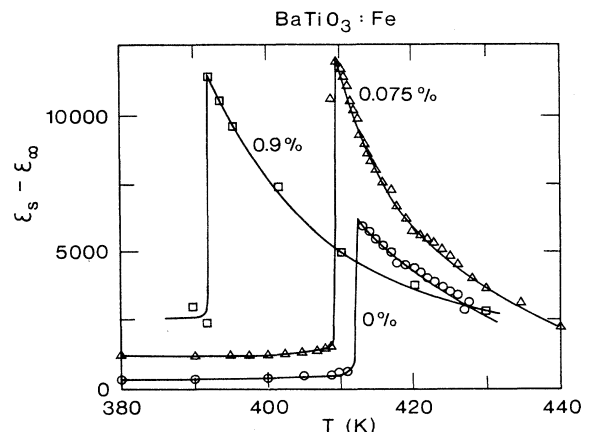


FIG. 3. Dispersion step $\epsilon_s - \epsilon_\infty$ vs temperature for pure and iron-doped BaTiO_3 . Doping level is indicated as a percentage. Solid lines are drawn to guide the eye.

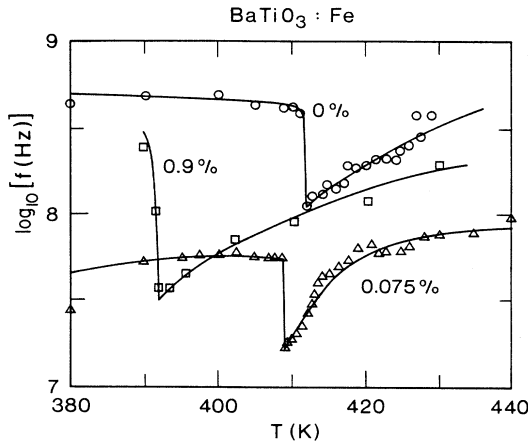


FIG. 4. Relaxation rate τ^{-1} as a function of temperature. Labels indicate iron doping percentage. Solid lines are drawn to guide the eye.

as in order-disorder ferroelectric triglycine sulfate¹³ and NaNO_2 .¹⁶ While in BaTiO_3 τ^{-1} is minimum at T_c , a fit of τ^{-1} to $A|T - T_c|$ is unsatisfactory: The changes of τ vs T in the accessible temperature range $|T - T_c| = 10$ K are small compared to the residual value of $\tau^{-1} = 10^8 \text{ s}^{-1}$ at T_c . It is plausible to assume that the relaxing species involves off-center Ti ions, displaced with respect to their centrosymmetric site. The displacement has been estimated to be 0.14 \AA on the basis of the paramagnetic resonance of Fe^{3+} on Ti sites⁶ and shown to drop by at least a factor of 3 at T_c . Independent hopping of Ti ions between symmetry-related wells would lead to a relaxation step of $\epsilon_s - \epsilon_\infty = nP^2/(3kT\epsilon_0) = 0.1$, far below the observed value of 6×10^3 . Here n is the number of Ti^{4+} ions per m^3 , P their local polarization $P = (4e)(0.14 \text{ \AA})$, and $\epsilon_0 = 8.85 \times 10^{-12} \text{ C/Vm}$. Coherent motion of clusters of size V_c leads to $\epsilon = \langle \delta P^2 \rangle V_c / kT$. On the basis of the estimate of $\langle \delta P^2 \rangle^{1/2} \leq 0.05 \text{ \AA}$ at T_c , we find $V_c \geq 4000 \text{ \AA}^3$. This value is between the one given¹⁷ on the basis of the photoelastic coupling $V_c = 40000 \text{ \AA}^3$ and the one based on a structural analysis $V_c = 1600 \text{ \AA}^3$ (assuming no lateral correlation, i.e., 4 \AA). More important than its actual size is its attribution to a relaxation mode. The fact that relaxation rates of the nuclear spin $^{49}\text{Ti}^{4+}$ and $^{47}\text{Ti}^{4+}$ in a range from T_c to $T_c + 10$ K determined by NMR techniques¹⁸ are equal to those seen by the dielectric method confirms that Ti^{4+} is involved in the local polar motion.

Attempts have also been made to resolve the dynamical polarization by light scattering. Detection of a relaxation mode in the cubic phase requires hyper-Raman spectroscopy, i.e., detection near 2ω . The spectra were shown to resolve an overdamped soft mode (or relaxation peak) of about $2 \text{ cm}^{-1} = 60 \text{ GHz}$.¹⁹ Because of the strong mode softening, the absolute determination of ϵ in this frequency range on the basis of light scattering is usually limited to temperatures higher than $T_c + 50$ K.¹⁴ Interestingly enough, conventional Raman scattering also resolves a relaxation peak,²⁰ although it should be symmetry forbidden. It was correctly concluded that this peak (which is

substantially broader than the hyper-Raman peak) owed its presence to disorder on the scale of the wavelength of light. We maintain, however, that the relaxation peaks seen in the optical measurements contain only a small fraction of the total dispersion probed in dielectric relaxation measurements. We find a strong monodispersive relaxation described by $\epsilon(10^6 \text{ Hz}) \approx 10^4$ and $\epsilon(10^{10} \text{ Hz}) \approx 700$, thus $\Delta\epsilon \approx 9.3 \times 10^3$. Since the optical relaxation peak is at 10^{11} Hz , and has a strength of less than $\frac{1}{10}$ of the one presented here, the question arises as to the interpretation of inelastic light scattering data in terms of precursor order of the polar transition.²⁰ In our view, the high frequency and the weak intensity of this phenomenon, as well as Arrhenius behavior associated with its dynamics, are evidence against this interpretation. It is interesting to compare this approach with that of Fontana, Ridah, and Kugel,²¹ who developed a model of coupled resonator and relaxation modes which was capable of describing both dielectric response and Raman activity in KNbO_3 .

Addition of Fe^{3+} enhances the relaxation strength of the strongest mode (reported here), slows it down and widens somewhat the distribution of relaxation times. It is natural to assume that this impurity, which is associated with oxygen vacancies, enhances the asymmetry of the potential for Ti^{4+} . (Accordingly, for $x_{\text{Fe}} \approx 7.5 \times 10^{-4}$, the Ti^{4+} displacement is larger than 0.14 \AA .⁶) The concomitant enhancement of the barrier height is then responsible for the (moderate) slowing down of the Ti^{4+} motion. One could argue that change of the correlation length, rather than Ti^{4+} displacement, accounted for the observed effect. Impurity-induced fields are, however, of random nature as evidenced by the distribution width $\Delta(\ln\tau)$. They have a tendency to reduce rather than to enhance polar correlation.²²

Since oxygen vacancies are present in BaTiO_3 even in the absence of Fe^{3+} doping, correlation of polar motion is restricted by random fields due to those vacancies. This would explain the noncriticality of the correlation volume as mentioned by Lines and Glass.¹⁶

IV. CONCLUSION

The susceptibility maximum in BaTiO_3 seen at the transition from the cubic to the tetragonal phase originates from a relaxation mode. Its predominant relaxation rate is equal to $\sim 10^8 \text{ s}^{-1}$ at T_c and the spread of the relaxation rate is less than one decade. It is associated with the hopping of off-center Ti ions between symmetry-related wells separated by 90° . Polar motion is coherent within volumes of 10^4 \AA^3 , which corresponds to 20-\AA linear distance. Iron doping slows down the motion to off-center Ti ions.

ACKNOWLEDGMENTS

It is our pleasure to thank Mr. Lompré for the supply of crystals, and G. Godefroy and K. Alex Müller for illuminating discussions. We acknowledge the technical assistance of P. Lunkenheimer.

- ¹M. E. Lines and A. M. Glass, *Principles and Applications of Ferroelectrics and Related Materials* (Clarendon, Oxford, 1977), p. 241.
- ²R. Comès, M. Lambert, and A. Guinier, *Solid State Commun.* **6**, 719 (1968).
- ³M. Lambert and R. Comès, *Solid State Commun.* **7**, 305 (1969).
- ⁴S. M. Shapiro, J. D. Axe, G. Shirane, and T. Riste, *Phys. Rev. B* **6**, 4332 (1974).
- ⁵M. E. Lines and A. M. Glass, *Principles and Applications of Ferroelectrics and Related Materials* (Clarendon, Oxford, 1977), p. 245.
- ⁶K. A. Müller, in *Nonlinearity in Condensed Matter*, edited by A. R. Bishop, D. K. Campbell, P. Kumar, and S. E. Trullinger, Springer Series in Solid State Physics, Vol. 69 (Springer-Verlag, Heidelberg, 1987), p. 234.
- ⁷*Landolt-Börnstein: Ferroelectric Oxides*, edited by K. H. Hellwege and A. M. Hellwege (Springer-Verlag, Berlin, 1981), Group 3, Vol. 16, Part a.
- ⁸R. Böhmer, M. Maglione, P. Lunkenheimer, and A. Loidl, *J. Appl. Phys.* **65**, 901 (1989).
- ⁹M. Maglione, Thesis No. 523, Ecole Polytechnique Fédérale de Lausanne, Switzerland, 1987.
- ¹⁰U. T. Höchli, *Phys. Rev. Lett.* **48**, 1494 (1982).
- ¹¹B. T. Matthias, C. E. Miller, and J. P. Remeika, *Phys. Rev.* **104**, 849 (1956); M. E. Lines and A. M. Glass, *Principles and Applications of Ferroelectrics and Related Materials* (Clarendon, Oxford, 1977), p. 321.
- ¹²H. Arend, in *Proceedings of the International Meeting on Ferroelectricity*, edited by V. Dvorák, A. Fouskova, and P. Gloger (Institute of Physics of the Czechoslovak Academy of Sciences, Prague, 1966), p. 231.
- ¹³T. S. Benedict and J. L. Durand, *Phys. Rev.* **109**, 1091 (1958).
- ¹⁴J. Petzelt, G. V. Kozlov, and A. A. Volkov, *Ferroelectrics* **73**, 101 (1987).
- ¹⁵F. D. Tischer, *Mikrowellen-Messtechnik* (Springer-Verlag, Berlin, 1958), p. 232.
- ¹⁶I. Hatta, *J. Phys. Soc. Jpn.* **24**, 1043 (1968); M. E. Lines and A. M. Glass, *Principles and Applications of Ferroelectrics and Related Materials* (Clarendon, Oxford, 1977), p. 327ff.
- ¹⁷M. E. Lines, *Phys. Rev. B* **5**, 3690 (1972).
- ¹⁸A. Hackmann, O. Kanert, H. Kolem, H. Schulz, K. A. Müller, and J. Albers (unpublished).
- ¹⁹M. Vogt, *Jpn. J. Appl. Phys. Suppl.* **24-2**, 112 (1985); K. Inoue and S. Akimoto, *Solid State Commun.* **46**, 441 (1983).
- ²⁰J. P. Sokoloff, L. L. Chase, and D. Rytz, *Phys. Rev. B* **38**, 597 (1988).
- ²¹M. D. Fontana, A. Ridah, and G. E. Kugel, *Phys. Status Solidi (b)* **147**, 441 (1988).
- ²²K. Binder and A. P. Young, *Rev. Mod. Phys.* **58**, 801 (1986).